

Low Threshold, Room Temperature Pulsed Operation of 1.5 μm Vertical-Cavity Surface-Emitting Lasers with an Optimized Multi-Quantum Well Active Layer

K. Uomi, S. J. B. Yoo, *Member, IEEE*, A. Scherer, R. Bhat, *Member, IEEE*, N. C. Andreadakis, *Senior Member, IEEE*, C. E. Zah, *Senior Member, IEEE*, M. A. Koza, and T. P. Lee, *Fellow, IEEE*

Abstract—Room temperature, pulsed operation of 1.5 μm vertical-cavity surface-emitting laser is demonstrated by the optimization of an InGaAs/InGaAsP multi-quantum well active layer, especially the number of quantum wells and the barrier thickness considering matched gain effect. Low threshold currents of 17 mA in $5 \times 7 \mu\text{m}^2$ -devices and 25 mA in $7 \times 10 \mu\text{m}^2$ -devices were achieved.

I. INTRODUCTION

VERTICAL-CAVITY surface-emitting lasers (VCSELs) [1] are attractive light sources including optical interconnections, fiber in the loop, and optical signal processing. In addition, VCSELs have advantages against edge-emitting lasers, such as wafer scale fabrication and testing, two-dimensional array fabrication, and monolithic optoelectronic integration. Up to now, there have been numerous reports on low threshold (< 1 mA), room-temperature (RT), CW operation of GaAs/GaAlAs and InGaAs/GaAs VCSELs at 0.85–0.98 μm [2]–[4]. However, in the wavelength range of 1.3–1.55 μm , suitable for optical fiber communication systems, only a few studies have demonstrated RT, pulsed operation (50 mA [5], 34 mA [6], 9 mA [7]) of VCSELs based on bulk active layer. Recently, RT, CW operation of 1.3 μm VCSEL was firstly reported [8]. Optimization of the laser structure, especially the active layer, in long-wavelength VCSELs is important in order to achieve low threshold operation, because of the existence of Auger recombination and intervalence-band absorption. In this letter, we report RT, pulsed operation of 1.5 μm VCSELs with a theoretically optimized InGaAs/InGaAsP multi-quantum well (MQW) active layer considering matched gain effect [9].

II. THEORETICAL DEVICE DESIGN

The optimization of MQW active layer in MQW-VCSELs, especially the number of quantum wells N_w and the barrier thickness L_b , will be discussed to achieve low threshold operation from the viewpoint of matched gain effect [9]. The threshold gain g_{th} and the threshold current density J_{th} of

MQW-VCSELs with internal loss and with matched gain effect, is given by

$$\xi_m N_w L_w g_{th} = \frac{1}{2} \ln \left(\frac{1}{R_f R_r} \right) + \sum_{w,b} \xi_m N_i L_i \alpha_i + \left(L_c - \sum_{w,b} N_i L_i \right) \alpha_c \quad (1)$$

$$\xi_m = 1 + \frac{\sin 2\pi\sigma}{2\pi\sigma}, \quad \sigma = \frac{1}{\lambda} \sum_{w,b} n_i L_i \quad (2)$$

$$J_{th} = e N_w L_w (B n_{th}^2 + C n_{th}^3) \quad (3)$$

where L_w is the well thickness, R_f , R_r are the reflectivities of the front and rear side mirrors, ξ_m is the gain matching factor [9], α_i , α_c are the absorption loss in the active and cladding layers, respectively, L_c is the cavity length, n_{th} is the threshold carrier density, B is the radiative coefficient, and C is Auger coefficient. The gain coefficient was obtained theoretically from the gain model, taking in account the k -selection rule and the polarization dependence of the dipole moment for band-to-band recombinations, which was described in detail elsewhere [10]. To estimate g_{th} and n_{th} for each N_w , eq. (1) was self-consistently solved considering the carrier density dependence of optical loss α_i due to free-carrier and intervalence-band absorption.

According to (1), a large N_w is desirable to increase the one-round-trip gain in the cavity. However, in order to achieve matched gain, the total MQW thickness should be thinner than one-half wavelength, which requires a reduction in N_w . Here, the importance of introducing thin barrier layers to overcome the above trade-off relation on N_w is discussed.

Fig. 1 shows an example of calculated N_w dependence of J_{th} in 1.55 μm unstrained MQW-VCSELs at various mean reflectivity $R (= \sqrt{R_f R_r})$. In the calculation, MQW active layer consists of 7-nm-thick InGaAs wells separated by 6-nm-thick InGaAsP barriers whose bandgap wavelength is 1.15 μm . Note that lowest J_{th} is achieved when total MQW layer thickness is between $\lambda/4n$ and $\lambda/2n$ (N_w : 8–17, especially $N_w = 12$), as is expected from matched gain effect [9]. Figure 2 shows the calculated L_b dependence of J_{th} for 1.55 μm unstrained and strained ($L_w = 3.5$ nm, $\Delta a/a = +1.0\%$)

Manuscript received September 9, 1993.

K. Uomi is with the Central Research Laboratory, Hitachi Ltd., Kokubunji, Tokyo 185, Japan.

S. J. B. Yoo, A. Scherer, R. Bhat, N. C. Andreadakis, C. E. Zah, M. A. Koza, and T. P. Lee are with Bell Communications Research, 331 Newman Springs Road, Red Bank, NJ 07701.

IEEE Log Number 9400083.

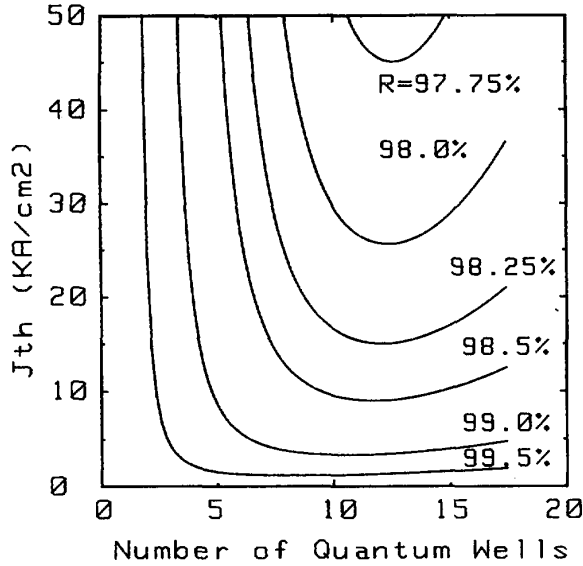


Fig. 1. Calculated N_w dependence of J_{th} in $1.55 \mu\text{m}$ unstrained InGaAs/InGaAsP MQW-VCSELs with well thickness of 7 nm and barrier thickness of 6 nm , at various mean reflectivity $R(= \sqrt{R_f R_r})$.

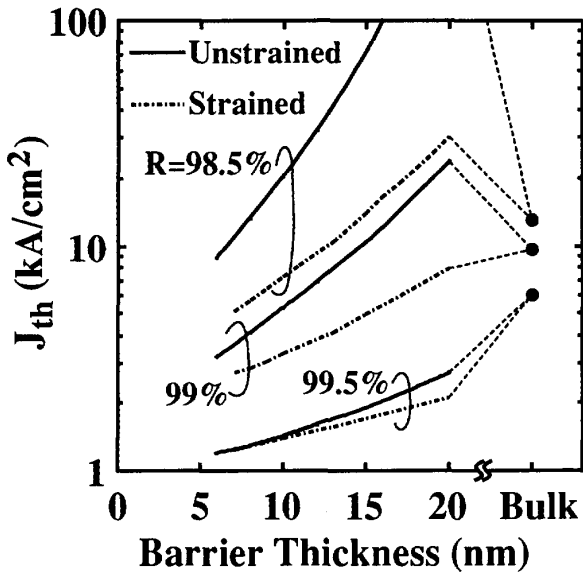


Fig. 2. Calculated L_b dependence of J_{th} for $1.55 \mu\text{m}$ unstrained and strained ($L_w = 3.5 \text{ nm}$, $\Delta a/a = +1.0\%$) MQW-VCSELs when N_w is optimized for each R . This figure also shows the calculated J_{th} of $1.55 \mu\text{m}$ bulk-VCSELs with an optimized active layer thickness.

MQW-VCSELs when N_w is optimized for each R . This figure also shows the calculated J_{th} of $1.55 \mu\text{m}$ bulk-VCSELs with an optimized active layer thickness. As is seen in this Fig. 2, it is found that J_{th} decreases with the decrease of L_b , which mainly results from the increase of one-round-trip gain due to a large confinement factor. However, L_b should be designed to be $5\text{--}6 \text{ nm}$ to reduce the coupling of two-dimensional electrons between neighboring wells [11]. Moreover, a lower J_{th} can be

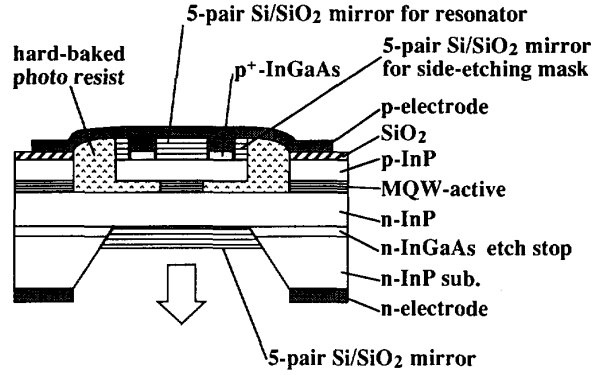


Fig. 3. Schematic structure of $1.5 \mu\text{m}$ MQW-VCSELs.

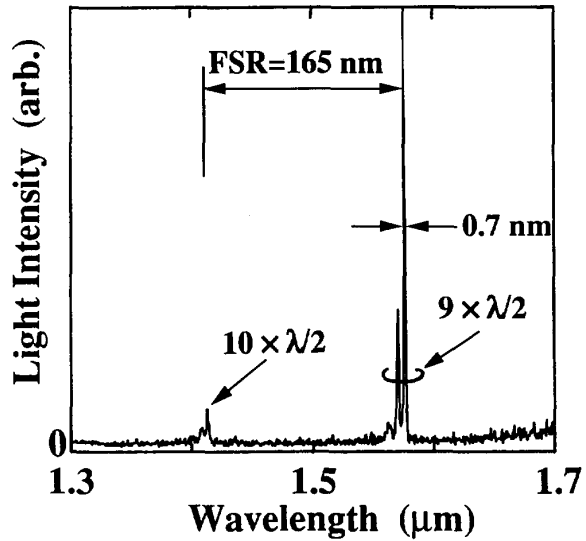


Fig. 4. Emission spectrum of a $5 \times 7 \mu\text{m}^2$ device under CW 2 mA current at room temperature.

expected in the optimized MQW-VCSELs, as compared with bulk-VCSELs, if R is larger than 98.5% .

III. EXPERIMENTAL

The schematic of $1.5 \mu\text{m}$ MQW-VCSELs used in this study is shown in Fig. 3. The VCSEL structures, grown on an n -type (001) InP substrate using organic metal chemical vapor epitaxy, consists of a $0.2 \mu\text{m}$ n -InGaAs etch-stop layer, a $0.65 \mu\text{m}$ n -InP cladding layer, an unstrained MQW active layer, a $0.98 \mu\text{m}$ p -InP cladding layer and a $0.2 \mu\text{m}$ p -InGaAs cap layer. The MQW active layer was theoretically optimized to be composed of twelve 7-nm InGaAs wells separated by 6-nm thick InGaAsP barriers, as discussed in the previous section. The MQW total thickness was about $3/4n\lambda$. The MQW layer was located at the peak of the optical standing wave to achieve matched gain.

The wafer was processed into the photo-resist-embedded mesa structure with an etched well structure. First, a 5-pair Si/SiO₂ diamond shaped mirror was formed on the

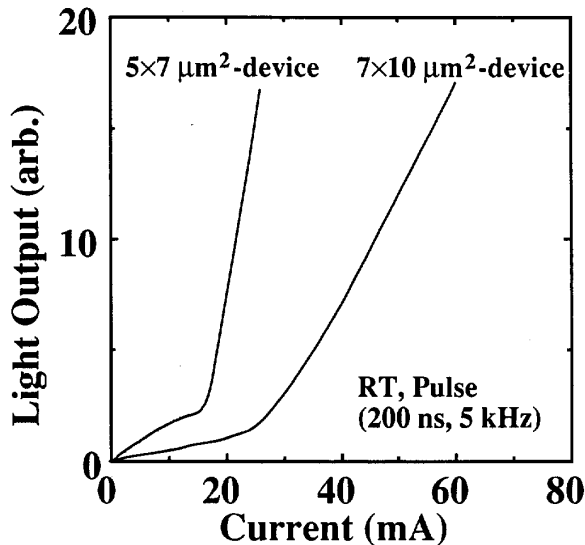


Fig. 5. Light-output power versus current characteristics (L-I) of 1.5 μm MQW-VCSELs with active area size of 5×7 and $7 \times 10 \mu\text{m}^2$ under pulsed operation (200 ns, 5 kHz) at room temperature.

p-InP cladding layer using reactive ion sputtering and a standard liftoff technique. Then, active areas were undercut into diamond shapes of 5×7 and $7 \times 10 \mu\text{m}^2$, using a selective etchant of $4\text{H}_2\text{SO}_4:1\text{H}_2\text{O}_2:1\text{H}_2\text{O}$ and dummy 5-pair Si/SiO₂ multi-layer as an etching mask. The diamond-shaped active layer was automatically formed by the larger etching-rate in the [010] direction than that in both the [011] and [01 $\bar{1}$] directions. This self-aligned process permits precise control of the position of the active area just below the p-side mirror. The size of p-side mirror was slightly larger than that of active layer in order not to decrease R . The VCSEL mesa was embedded in hard-baked photo-resist and Ti/Pt/Au was evaporated to form a p-type electrode. Next, a short cavity structure ($2 \mu\text{m} \sim 9 \times \lambda/2n$) was formed by selectively removing the n-InP substrate after evaporating a AuGeNi electrode to the n-side surface. Finally, a 5-pair Si/SiO₂ mirror was deposited on the bottom of the etched well using reactive ion sputtering. The reflectivity of the mirrors was estimated to be 99.2% [12]. The devices were bonded p side-down on a Au-coated Cu heat sink with an In solder. The laser light was detected from the n-mirror side.

Fig. 4 shows the emission spectrum of a $5 \times 7 \mu\text{m}^2$ device under CW 2 mA current at RT. Two longitudinal modes with mode spacing (FSR) of 165 nm was clearly observed. The value of FSR is in good agreement with the calculated one using device parameters. The Finesse value evaluated from FSR and spectral width (0.7 nm) is about 240, which corresponds to one-round-trip R_{total} of 98.7%. The difference between R and R_{total} was 0.5%, which resulted from the diffraction loss in clad layers and the scattering loss in active layer. The device resistances were 130 and 90 Ω for 5×7 and $7 \times 10 \mu\text{m}^2$ devices, respectively. Fig. 5 shows light-output power versus current characteristics (L-I) for 1.5 μm MQW-

VCSELs with active area size of 5×7 and $7 \times 10 \mu\text{m}^2$ under pulsed operation (200 ns, 5 kHz) at RT. Lasing actions were observed in $5 \times 7 \mu\text{m}^2$ devices with threshold current I_{th} of 17 mA and in $7 \times 10 \mu\text{m}^2$ devices with I_{th} of 25 mA. The J_{th} was estimated to be 50 and 35 kA/cm^2 for 5×7 and $7 \times 10 \mu\text{m}^2$ devices, respectively, which was about 5 times higher than theoretically predicted values in Figs. 1 & 2. This discrepancy may be caused by nonuniform current injection into the active layer [13], which results from lateral diffusion in both the p and n cladding layers.

IV. CONCLUSION

In conclusion, we have demonstrated first lasing operation of current-injection-type long-wavelength MQW-VCSELs. This was mainly attributed to the optimization of an MQW active layer, especially the number of quantum wells and the barrier thickness, in order to achieve matched gain and to increase one-round-trip gain.

REFERENCES

- [1] K. Iga, F. Koyama, and S. Kinoshita, "Surface emitting semiconductor lasers," *IEEE J. Quantum Electron.*, vol. QE-24, pp. 1845-1855, 1988.
- [2] J. L. Jewell, J. P. Harbison, A. Scherer, Y. H. Lee, and L. T. Florez, "Vertical-cavity surface-emitting lasers: design, growth, characterization," *IEEE J. Quantum Electron.*, vol. QE-27, pp. 1332-1346, 1991.
- [3] R. S. Geels, S. W. Corzine, and L. A. Coldren, "InGaAs vertical-cavity surface-emitting lasers," *IEEE J. Quantum Electron.*, vol. QE-27, pp. 1359-1367, 1991.
- [4] A. Scherer, M. Walther, J. P. Harbison, and L. T. Florez, "Fabrication of low threshold voltage micro lasers," *Electron. Lett.*, vol. 28, pp. 1224-1226, 1992.
- [5] H. Wada, D. I. Babic, D. L. Crawford, J. J. Dudley, J. E. Bowers, E. L. Hu, J. L. Merz, and M. G. Young, "Low-threshold, high-temperature pulsed operation of InGaAs/InP vertical cavity surface emitting lasers," *IEEE Photon Technol. Lett.*, vol. 3, pp. 977-979, 1991.
- [6] T. Baba, Y. Yogo, K. Suzuki, F. Koyama, and K. Iga, "Low threshold room temperature pulsed and -31°C CW operations of 1.3 mm GaInAsP/InP buried heterostructure surface emitting lasers," in *Tech. Dig., OFC'93*, San Jose, CA, Paper PD28-1, 1993.
- [7] J. J. Dudley, D. I. Babic, R. Mirin, L. Yang, B. I. Miller, R. J. Ram, T. Reynolds, E. L. Hu, and J. E. Bowers, "Low threshold, electrically injected InGaAsP (1.3 mm) vertical cavity lasers on GaAs substrate," in *Tech. Dig., 51st Annual Device Research Conference*, Santa Barbara, CA, Paper III B-, 1993.
- [8] T. Baba, Y. Yogo, K. Suzuki, F. Koyama, and K. Iga, "First room temperature CW operation of GaInAsP/InP surface emitting laser," in *Tech. Dig., Topical meeting on Quantum Optoelectronics*, Palm Springs, CA, Paper PD2-2, 1993.
- [9] S. W. Corzine, R. S. Geels, J. W. Scott, R. Yan, and L. A. Coldren, "Design of Fabry-Perot surface emitting lasers with a periodic gain structure," *IEEE J. Quantum Electron.*, vol. QE-25, pp. 1513-1524, 1989.
- [10] K. Uomi, M. Aoki, T. Tsuchiya, and A. Takai, "Dependence of high-speed properties on the number of quantum wells in 1.55 μm InGaAs-InGaAsP MQW $\lambda/4$ -shifted DFB laser," *IEEE J. Quantum Electron.*, vol. QE-29, pp. 355-360, 1993.
- [11] K. Uomi, M. Aoki, T. Tsuchiya, and M. Suzuki, "High-speed properties of 1.55 μm InGaAs-InGaAsP MQW $\lambda/4$ -shifted DFB lasers," in *Proc. SPIE, OE/LASE '92 Conference on Laser Diode Technology and Application IV*, Los Angeles, CA, Paper 1634-13, 1992, (SPIE, vol. 1634, Laser Diode Technology and Application IV, pp. 110-118, 1992).
- [12] S. J. B. Yoo, R. Bhat, A. Scherer, K. Uomi, C. E. Zah, M. A. Koza, M. C. Wang, and T. P. Lee, "Quasi-CW room-temperature operation of 1.55 μm vertical cavity surface emitting lasers grown by OMCVD," in *Tech. Dig. IEEE/LEOS '92 Annual meeting*, post-deadline paper PD-6, 1993.
- [13] H. Wada, D. I. Babic, M. Ishikawa, and J. E. Bowers, "Effects of nonuniform current injection in InGaAsP/InP vertical cavity lasers," *Appl. Phys. Lett.*, vol. 60, pp. 2974-2976, 1992.